Tunable thermo-phototronic effect in unintentionally doped n-3C–SiC/p-Si heterostructure ⊘

Hung Nguyen ✉ 📵 ; Duy Van Nguyen 📵 ; Thi Lap Tran 📵 ; Pingan Song; Min Hong; Dzung Viet Dao 📵 ;
Nam-Trung Nguyen 📵 ; John Bell 📵 ; Toan Dinh ✉

Check for updates

View Online   Export Citation

Tunable thermo-phototronic effect in unintentionally doped n-3C–SiC/p-Si heterostructure

Hung Nguyen,[1,2,a] (iD) Duy Van Nguyen,[1,2] (iD) Thi Lap Tran,[1,2] (iD) Pingan Song,[1,2] Min Hong,[1,2] Dzung Viet Dao,[3] (iD) Nam-Trung Nguyen,[3] (iD) John Bell,[1,2] (iD) and Toan Dinh[1,2,a]

AFFILIATIONS

[1]School of Engineering, University of Southern Queensland, Toowoomba, Queensland 4350, Australia
[2]Centre for Future Materials, University of Southern Queensland, Toowoomba, Queensland 4350, Australia
[3]Queensland Micro- and Nanotechnology Centre, Griffith University, Nathan, Queensland 4111, Australia

[a]Authors to whom correspondence should be addressed: hung.nguyen@unisq.edu.au and toan.dinh@unisq.edu.au

ABSTRACT

The convergence of the Internet of Things (IoT) and 5G technology is creating a high demand in sensor signals, prompting a shift toward self-powered sensors as eco-friendly alternatives to the conventional battery-powered ones. The 3C–SiC/Si heterostructure recently has gained significant attention for sensing applications, including self-powered sensors. However, it has remained unclear about the sensing properties and the underlying physics of the sensing mechanism of the unintentionally doped n-SiC/p-Si heterostructure, hindering the design optimization of SiC/Si heterojunction self-powered devices for diverse applications. This study investigates the thermo-phototronic effect and its underlying mechanism in an unintentionally doped n-3C–SiC/p-Si heterostructure for self-powered sensors. The sensors can be self-powered by absorbing energy from photons to generate photovoltage and photocurrent as high as 110 mV and 0.8 μA. In addition, widening the electrode spacing increased the photovoltage of the device by as much as 122% and the photocurrent by as much as 65%. When the temperature gradient is progressively increased by heating one electrode, the photovoltage decreases gradually, while the current exhibits an initial increase of up to 10%, followed by a decline. These tunable characteristics are attributed to the capability of the heterostructure to control the transport of charge carriers and the impact of unintentionally doped n-SiC on the diffusion of charge carriers. The results of this study can be applied in the development of photodetectors, thermal sensors, and position detectors with tunable sensing performance.

Published under an exclusive license by AIP Publishing. https://doi.org/10.1063/5.0187276

Temperature sensing and photo detecting play significant roles in the application of the sensor. However, the thermoelectric effect, the pyroelectric effect, and the photovoltaic effect have been intensively investigated but still have some limitations.[1–4] Thermo-phototronic effect recently has drawn a lot of attention and shown promising potential for simultaneously detecting light and temperature.[5,6] The synergy between thermal-electric and photovoltaic effects enables the sensors to produce very responsive and accurate electric signals.[7]

There have been several reports regarding the thermo-phototronic effect for P$_3$HT/ZnO, Na-doped SnS, BiFeO$_3$, and InP/ZnO heterostructure.[8–11] However, the fabrication of the mentioned materials still has some challenges. Instead, 3C–SiC/Si heterostructure has received interest because it has a large bandgap, good chemical inertness, and great sensing behavior.[12,13] Additionally, the fabrication of 3C–SiC/Si heterostructures has many advantages, such as starting

from the commercially available low-cost silicon wafers. Regarding thermal-electric and photovoltaic effects, many reports are showing that the 3C–SiC/Si heterostructures can capture photons to power themselves for use in supersensitive sensors.[14–18] We have shown that applying temperature gradient can significantly change the electrical properties in highly doped n-3C–SiC/p-Si heterostructures.[7,14] However, the thermo-phototronic effect in the unintentionally doped n-3C–SiC/p-Si heterostructures has yet to be clear. However, some materials have been proven to exhibit tunable single optoelectronic or thermoelectric effects.[19–22] To date, no heterojunction has demonstrated a tunable thermo-phototronic effect using a temperature gradient induced by one-sided horizontal heating conditions.

In this study, we investigated thermo-phototronics of an unintentionally doped n-3C–SiC/p-Si heterostructure by examining the impact of temperature gradients and electrode spacing on the lateral

optoelectronic effect of the heterostructure. Our results show that the device is self-powered and exhibits tunable thermo-phototronic properties with photovoltage and photocurrent values as high as 110 mV and 0.8 μA, respectively. We found that increasing the temperature gradient (by heating one electrode) reduced the output voltage and current in general for the unintentionally doped n-3C–SiC/p-Si heterostructure. Notably, the drop for 2 mW/cm² light intensity is higher than the drop for 5 mW/cm² light intensity. Furthermore, progressively increasing the gap between the measured electrodes from 1.5 to 9 mm can enhance the voltage and current by up to 122% and 65%, respectively.

Figure 1(a) illustrates the fabrication process of the device. The sensor was fabricated using a photolithography process to obtain suitable shapes for characterization. Figure 1(b) shows an AFM picture of the SiC film over an area measuring $5 \times 5 \ \mu m^2$. The root mean square of the AFM image is measured at 1.08 nm, indicating the even growth of the SiC layer. Figure 1(c) shows an image of the device with Al electrodes A, B, C, and D positioned on top of the SiC layer. Figure 1(d) presents the I-V characterization of the device with gap sizes between the measured electrodes of 1.5, 4.5, and 9 mm. The I–V curves exhibit linearity, indicating Ohmic contact in the measurements. It is well known that SiC is blind to visible light.[23] Therefore, no local potential is generated in the SiC layer under light illumination.[24] As demonstrated in our recent works, the voltage in the SiC/Si heterostructure is established by the heterojunction, rather than on the SiC surface layer.[12,16] In our current work, we measured the lateral voltage using two electrodes from the surface of SiC.[13,18,25]

Figure 2 shows the repeatability in the photovoltage (a) and photocurrent (b) of the device with a 1.5 mm gap between electrodes under laser beam illumination. The wavelength of the laser beam is 635 nm. The power of the laser beams was 1 and 2.5 mW, while the illuminated

area was fixed at 0.5 cm², resulting in light intensities of 2 and 5 mW/cm². The laser beam was manually switched ON and OFF five times, each time for 20 s. In the absence of illumination, the recorded voltages and currents were almost nil. Upon illumination, both photovoltage and photocurrent immediately increased, demonstrating excellent repeatability throughout the test periods. This responsiveness and stability in the signals indicate the laser beam's suitability as a reliable energy source for the device. The generation of photovoltage can be explained by the theory of lateral illumination in a heterostructure shown in Fig. 2(c). The heterojunction plays an important role in boosting the photovoltage. The device response is reversable and highly stable in the dark condition and under illumination of visible lights.[15,18] Since the laser beam has a wavelength of approximately 635 nm (1.95 eV), photons can penetrate the 3C–SiC layer (energy bandgap of 2.3 eV) and be absorbed in the SiC layer (bandgap of 1.12 eV), resulting in the generation of electron–hole pairs (EHPs) within the Si layer. The built-in electric field E_0 in the heterostructure, formed by the n-SiC and p-Si layers, causes the electrons in the EHPs to be driven toward the SiC layer, while the holes are driven toward the Si layer. As a result, the heterojunction enhances the difference in electron concentration between the electrodes, boosting the photovoltage. As the light intensity increases from 2 to 5 mW/cm², more photons are injected into the Si layer and create additional EHPs. Consequently, more electrons are pushed toward the SiC layer. The increase in the number of electrons in the illuminated area of the SiC layer amplifies the electron gradient between the two electrodes, resulting in an augmented photovoltage measurement. We conducted KPFM measurements to observe the surface potential when the device is non-uniformly illuminated (supplementary material Fig. 1). The image reveals a gradient in surface potential under non-uniform illumination, confirming that light can indeed influence the potential and voltage across the heterostructure.
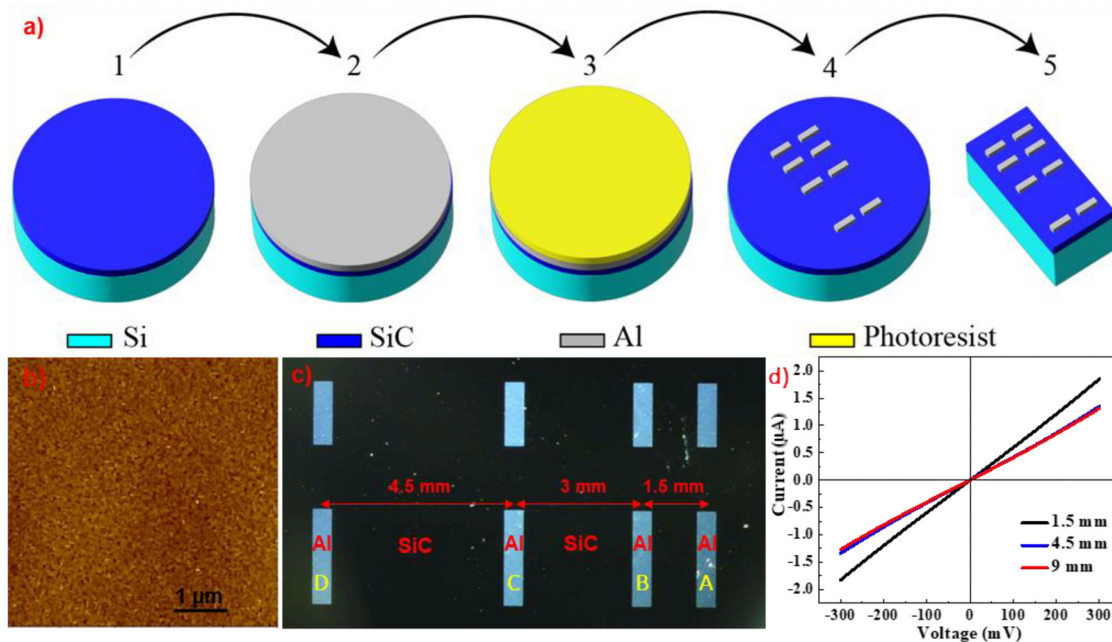
FIG. 1. (a) Fabrication process. (b) AFM image. (c) Picture of the device. (d) IV curves of the device in dark conditions of different electrode spacings.
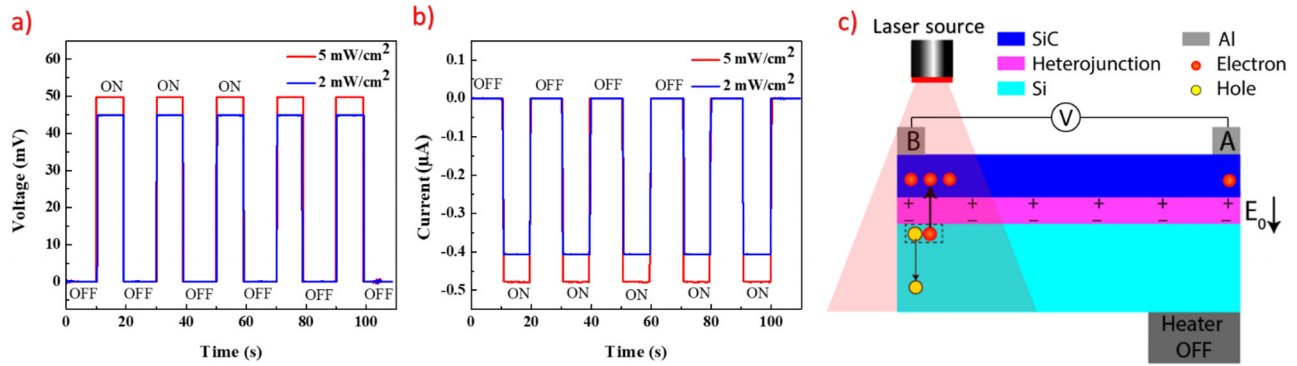
FIG. 2. (a) Response voltage, (b) response current, and (c) illustration of the mechanism of light energy conversion to electrical energy in the heterostructure.

Figure 3 shows the voltage and current response of the unintentionally doped n-SiC/p-Si heterostructure under a 635 nm laser beam of 2 and 5 mW/cm^2 intensities. The temperature gradient was initially stabilized at 0 K for 30 s and then gradually increased and held constant at 0.2, 0.4, 0.6, 0.8, and 1 K for another 30 s at each temperature. The temperature gradients were determined by subtracting the temperature of the hotter electrode from that of the colder electrode. Additional details regarding the temperature gradient and the temperatures of the electrodes can be found in supplementary material Table I. The charts in Figs. 3(a) and 3(b) show that the generated voltage and current remained stable when the temperature gradient between

electrodes A and B (ΔT_{AB}) was maintained, indicating that the effect of ΔT_{AB} on the generated voltage and current is consistent. When ΔT_{AB} is 0 K, the photovoltages are approximately 45 and 50 mV for 2 and 5 mW/cm^2, respectively. In Fig. 3(c), the voltage gradually drops as ΔT_{AB} increases, while in Fig. 3(d), the current initially increases by 5%–10% before decreasing. These tunable characteristics are further discussed in the following sections.

The temperature gradient can be employed to tune the sensitivity of device. When ΔT_{AB} was increased by heating electrode A, the temperature across the device was also increased. The measured voltage gradually decreases by increasing ΔT_{AB}, from 50 to 17 mV for 5 mW/cm^2
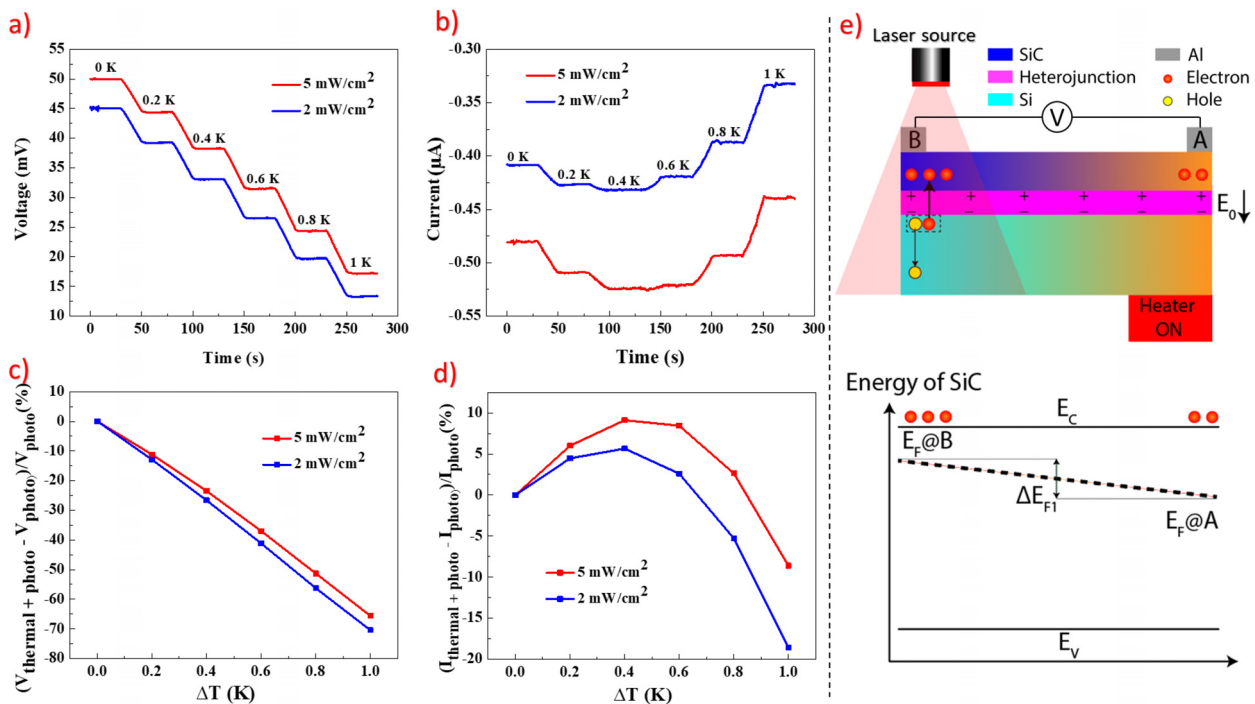
FIG. 3. The effect of the temperature gradient on the optoelectronic effect when the electrode spacing is 1.5 mm, by heating electrode A and illuminating electrode B: (a) response voltage; (b) response current; (c) enhancements in voltage by ΔT_{AB}; (d) enhancements in current by ΔT_{AB}; and (e) the interplay between photonic and thermal stimulation in the band structure of 3C–SiC.

illumination, and from 45 to 13 mV for 2 mW/cm². The proportion of change in voltage is described in Fig. 3(c). When gradually increasing ΔT_{AB} from 0 to 1 K, the measured voltage gradually decreased by 70% and 65% for 2 and 5 mW/cm² light intensities, respectively. The percentage of drop for 2 mW/cm² illumination is always higher than 5 mW/cm² as shown in Fig. 3(c). The mechanism of the voltage drop is shown in Fig. 3(e). When applying a temperature gradient to electrode A, the electron gradient in the SiC layer is primarily influenced by the diffusion of charge carriers and minimally by the Seebeck effect.[26] Since the Seebeck effect increases with the doping concentration, the unintentionally doped n-SiC layer has a concentration of approximately 10^{17} cm^{-3}, much lower than the high concentration of 10^{19} cm^{-3} in the highly doped n-SiC.[7] Therefore, the impact of the Seebeck effect on the voltage in the unintentionally doped SiC is much lower than that in the highly doped one. The diffusion of charge carriers is governed by Fick's law: $\Gamma_n = -D_n \times \Delta_n/dx$, where Γ_n is the flow of electrons, D_n is the coefficient of diffusivity, and Δ_n/dx is the electron gradient.[26,27] The use of unintentionally doped n-SiC layer with a low carrier concentration of approximately 10^{17} cm^{-3} will result in a low diffusion of carriers in the n-SiC layer, leading to a higher lateral voltage measured under the same light illumination (Fig. 2) compared to that measured in the highly doped n-SiC.[7]

In addition, the diffusion is altered by random thermal motion and scattering: $D_n = \nu_{th} \times \tau_m$, where ν_{th} is the thermal velocity and τ_m is the mean free time.[27] Because ν_{th} increases with temperature, the diffusion of electron increases with temperature. This results in a reduction of the electron gradient between the electrodes when temperature was increased.[27] This reduction leads to a decrease in the measured voltage between the two electrodes.

While the electron gradient for the 5 mW/cm² is higher compared to 2 mW/cm², the number of electrons generated from heating and the reduction in electron mobility could be comparable with those from illumination intensities. Therefore, the percentage of drop in voltage of 5 mW/cm² was smaller than 2 mW/cm² under the same temperature as shown in Fig. 3(c). Increasing the temperature can also slightly boost the current by the diffusion of charge carriers and stimulating electrons from donor levels to the conduction band.[27] However, because the current depends on the electron gradient between the two electrodes. Therefore, increasing the temperature reduces the electron gradient and voltage between the measured electrodes, resulting in an overall reduction in current. Furthermore, because a higher percentage drop in voltage leads to a more significant reduction in current, the percentage drop in current for 2 mW/cm² is greater than that for 5 mW/cm², as shown in Fig. 3(d).

When changing the illumination position from electrode B to electrode A while maintaining the same light intensity, we recorded similar values of photovoltage and photocurrent. The voltage and current also remain stable when ΔT_{AB} is kept constant, as shown in supplementary material Figs. 2(a) and 2(b). When the heater was deactivated, the voltage remained stable at 45 mV for 2 mW/cm² and 50 mV for 5 mW/cm². When the heater was activated, the temperature gradient was progressively increased from 0 to 1 K, the voltage gradually dropped to approximately 70% and 65% for 2 and 5 mW/cm² light intensities, respectively [supplementary material Fig. 2(c)]. This percentage drop in voltage closely matches the reduction observed when illuminating electrode B and heating electrode A, which confirms that the diffusion of charge carriers predominantly influenced the decrease

in the voltage value. The drop in voltage results in the drop in current [supplementary material Fig. 2(d)]. The effect of temperature gradient on the band structure of SiC and its mechanism are shown in supplementary material Fig. 2(e). Increasing the temperature at electrode A leads to a reduction in the electron concentration, resulting in a decrease in both the measured voltage and the difference in the Fermi level between the two electrodes.

Since electrode spacing has also had an impact on the photovoltage of the SiC/Si heterostructures,[28] we investigated the influence of electrode spacing on the thermo-phototronic behavior in the device by varying the gap to 4.5 and 9 mm. For 4.5 mm electrode spacing, the recorded voltage and current are very stable as shown in supplementary material Figs. 3(a) and 3(b). In supplementary material Fig. 3(c), the voltage drops from 82 to 19 mV as the temperature gradient increases from 0 to 2.2 K. Additionally, the current increases by roughly 5% when the temperature difference between A and C electrodes (ΔT_{AC}) is 0.9 K [supplementary material Fig. 3(d)], but it gradually decreases as ΔT_{AC} increases to 2.2 K (temperature at electrode A is 347.65 K). More details for the temperature gradient and temperature of the electrodes can be found in supplementary material Table I.

When changing the illumination position from electrode C to electrode A, the voltage also gradually decreased with an increase in the ΔTAC [supplementary material Figs. 4(a) and 4(c)]. The current increased slightly, peaking at a 4.1% increase at $\Delta T_{AC} = 0.9$ K and then gradually decreased with a further increase in the temperature of electrode A [supplementary material Figs. 4(b) and 4(d)]. Differences in voltage and current responses with a 4.5 mm electrodes gap when changing the illumination position were negligible, confirming that the Fick's law dominated the behavior of the device over the Seebeck effect.

The trend in voltage and current responses also persists as the electrode spacing widens to 9 mm. When illuminating electrode D and heating electrode A, the voltage and current remain stable when the temperature is kept constant, as shown in Figs. 4(a) and 4(b). The measured voltages are 110 and 100 mV at 0 K for light intensities of 5 and 2 mW/cm², respectively. As we gradually increase ΔT_{AD} from 0 to 3.6 K by incrementally raising the temperature of electrode A from 300.85 to 347.65 K, the voltages progressively decrease to 32.3 and 25.1 mV for 5 and 2 mW/cm², respectively. These reductions represent a 70% and 75% drop, as shown in Fig. 4(c). Regarding the current, there is a slight initial increase, followed by a gradual decrease, as shown in Fig. 4(d). The influence of ΔT_{AD} and the expansion of electrode spacing on the band structure of SiC and its mechanisms are depicted in Fig. 4(e).

Changing the illumination area from electrode D to electrode A does not affect the voltage and current response. The voltage gradually decreases with the increase in the temperature gradient, while the current initially experiences a slight increase before gradually decreasing with the rising temperature gradient due to heating. For more details, refer to supplementary material Fig. 5.

We have observed the excellent stability of the unintentionally doped n-SiC/p-Si heterostructure devices under repeated red laser illuminations (supplementary material Fig. 6) thanks to the excellent electronic properties of both SiC and Si. In addition, the voltages under green LED and red LED illumination were also extremely stable (supplementary material Fig. 7).

Notably, widening the electrode gap from 1.5 to 9 mm in Fig. 5(a) increases photovoltage by up to 122% and photocurrent by up to 65%,
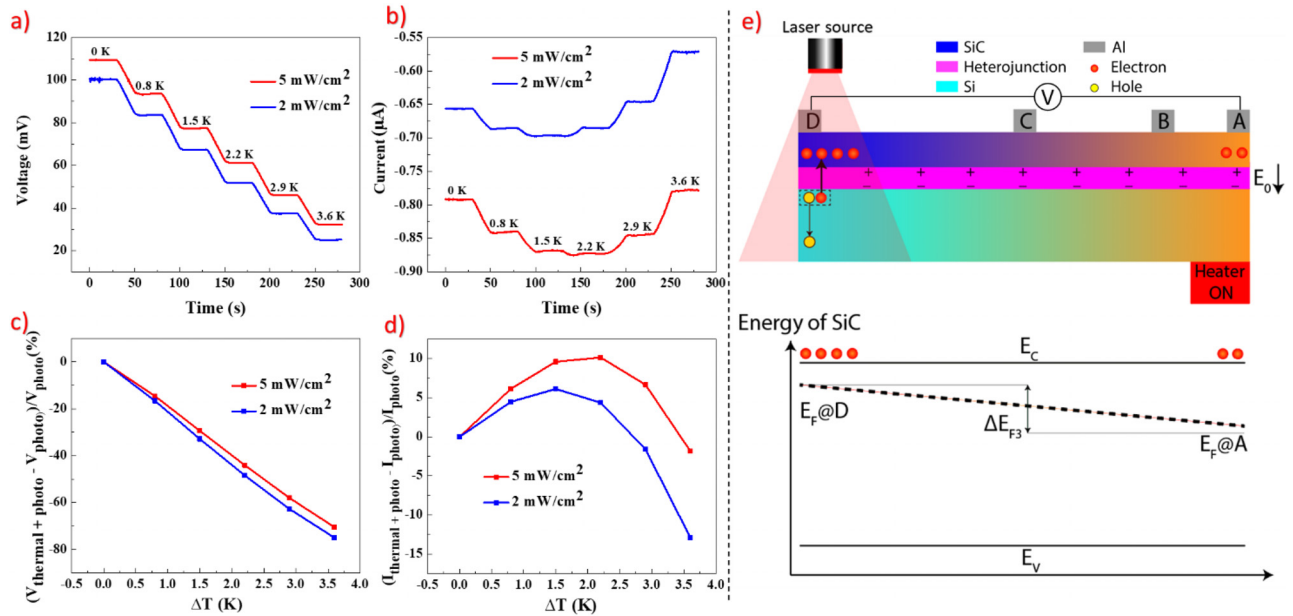
FIG. 4. The response when the gap between two electrodes is 9 mm, achieved by heating electrode A and illuminating electrode D: (a) voltage; (b) current; (c) enhancements in voltage by ΔT_{AD}; (d) enhancements in current by ΔT_{AD}; and (e) the interplay between photonic and thermal stimulation in the band structure of 3C–SiC.

confirming their enhancement with increasing electrode gap. When an electrode is illuminated, a high electron concentration forms around it, while the electron concentration around the non-illuminated electrode remains low, resulting in electron diffusion from the illuminated electrode to the non-illuminated electrode. According to Fick's law, the flow of diffusive electrons, represented by Γ_n, is inversely proportional to the distance dx. Consequently, when the electrode gap increases from 1.5 to 9 mm, the non-illuminated electrode with a 9 mm gap receives fewer electrons through diffusion compared to the one with a 1.5 mm gap. Therefore, the electron concentration and Fermi level in the non-illuminated electrode with a 9 mm gap are lower than those in the 1.5 mm gap electrode, creating an increased electron gradient and voltage as illustrated in Fig. 4(e). The higher electron gradient and voltage led to a current increase of up to 65%, as demonstrated in Fig. 5(b). The results show that the device's sensitivity can be tuned by changing the spacing or temperature gradient between the electrodes, providing flexibility to meet various requirements for tunable photodetection, temperature sensing, and position detection.

We observed the remarkable responsiveness and stability of unintentionally doped n-3C–SiC/p-Si heterostructure under light illumination. We demonstrated that progressively applying temperature gradient can tune the thermo-phototronic effect with a photocurrent up to 10%, while it gradually decreases the measured photovoltage from the unintentionally doped n-SiC/p-Si heterostructure. Additionally, widening the electrode gap can result in a photovoltage increase of up to 122% and a photocurrent increase of up to 65%. The responsivity was as high as 750 V/W. These results are comparable or better to those of other materials and structures (see supplementary material Table II). These results are

attributed to the capability of the unintentionally doped n-SiC/p-Si to control the transport of charge carriers on the diffusion process. These findings hold the potential to significantly enhance the knowledge within the field and advance the development of highly sensitive tunable self-powered sensors including photodetectors, temperature sensors, and position detectors.
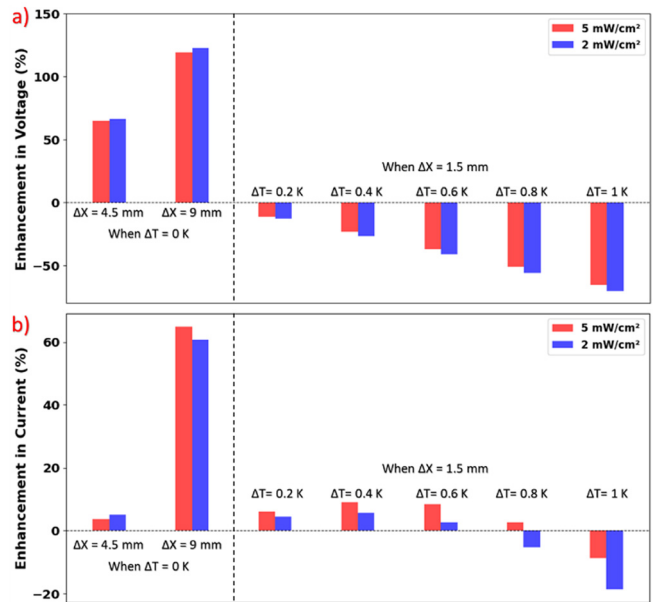
FIG. 5. Enhancement when increasing electrode gap (ΔX) and temperature gradient (ΔT), compared to when ΔX = 1.5 mm and ΔT = 0xyqK: (a) voltage and (b) current.

See the supplementary material for details of temperature gradient with respective electrode temperatures (supplementary material Table I); comparative table with other materials (supplementary material Table II); surface potential image (supplementary material Fig. 1); 1.5 mm electrode spacing: heating and illuminating electrode A (supplementary material Fig. 2); 4.5 mm electrode spacing: heating electrode A and illuminating electrode C (supplementary material Fig. 3); 4.5 mm electrode spacing: heating and illuminating electrode A (supplementary material Fig. 4); 9 mm electrode spacing: heating electrode A and illuminating electrode D (supplementary material Fig. 5); the stability of signal over time (supplementary material Fig. 6); and the stability of signal under different illuminating conditions (supplementary material Fig. 7)

AUTHOR DECLARATIONS
Conflict of Interest

The authors have no conflicts to disclose.

Author Contributions

Hung Nguyen: Data curation (equal); Formal analysis (equal); Investigation (equal); Validation (equal); Writing – original draft (equal). **Duy Van Nguyen:** Resources (supporting); Writing – review & editing (supporting). **Thi Lap Tran:** Conceptualization (supporting); Resources (supporting). **Pingan Song:** Resources (supporting); Writing – review & editing (supporting). **Min Hong:** Validation (supporting); Writing – review & editing (equal). **Dzung Viet Dao:** Funding acquisition (lead); Project administration (equal). **Nam Trung Nguyen:** Funding acquisition (equal); Resources (lead). **John Bell:** Resources (lead); Supervision (lead). **Toan Dinh:** Funding acquisition (equal); Resources (equal); Supervision (equal); Writing – review & editing (equal).

DATA AVAILABILITY

The data that support the findings of this study are available from the corresponding authors upon reasonable request.

REFERENCES

[1] H. Zhao, B. Ouyang, L. Han, Y. K. Mishra, Z. Zhang, and Y. Yang, Sci. Rep. **10**(1), 11864 (2020).
[2] Z. Wang, R. Yu, C. Pan, Z. Li, J. Yang, F. Yi, and Z. L. Wang, Nat. Commun. **6**(1), 8401 (2015).
[3] M. Kumar and H. Seo, Adv. Mater. **34**(5), 2106881 (2022).
[4] L. Wu, Y. Ji, B. Ouyang, Z. Li, and Y. Yang, Adv. Funct. Mater. **31**(17), 2010439 (2021).
[5] L. Yang, L. Wu, L. Su, L. Xu, L.-D. Zhao, and Y. Yang, Nano Energy **107**, 108140 (2023).
[6] T. Gao, Y. Ji, and Y. Yang, Adv. Mater. Technol. **5**(7), 2000176 (2020).
[7] H. Nguyen, T. Nguyen, D. V. Nguyen, H.-P. Phan, T. K. Nguyen, D. V. Dao, N.-T. Nguyen, J. Bell, and T. Dinh, ACS Appl. Mater. Interfaces. **15**(32), 38930–38937 (2023).
[8] J. Qi, N. Ma, X. Ma, R. Adelung, and Y. Yang, ACS Appl. Mater. Interfaces **10**(16), 13712–13719 (2018).
[9] K. Zhang and Y. Yang, Adv. Funct. Mater. **27**(38), 1703331 (2017).
[10] B. Ouyang, W. He, L. Wu, L.-D. Zhao, and Y. Yang, Nano Energy **88**, 106268 (2021).
[11] B. Ouyang, K. Zhang, and Y. Yang, Adv. Mater. Technol. **2**(12), 1700208 (2017).
[12] T. Dinh, T. Nguyen, A. Foisal, H.-P. Phan, T.-K. Nguyen, N.-T. Nguyen, and D. Dao, Sci. Adv. **6**(22), 2671 (2020).
[13] A. R. M. Foisal, T. Nguyen, T. Dinh, T. K. Nguyen, P. Tanner, E. W. Streed, and D. V. Dao, ACS Appl. Mater. Interfaces **11**(43), 40980–40987 (2019).
[14] H. Nguyen, T. Nguyen, D. Van Nguyen, H.-P. Phan, N.-T. Nguyen, D. Dao, J. Bell, and T. Dinh, "Thermo-phototronic Effect for self-powered photodetector using n-3C-SiC/p-Si heterostructure," *2022 IEEE Sensors* (IEEE, Dallas, TX, 2022). pp. 1–4 .
[15] T. Nguyen, T. Dinh, H. Nguyen, T. H. Vu, C.-D. Tran, P. Song, J. Bell, N.-T. Nguyen, and D. V. Dao, Nano Energy **96**, 107030 (2022).
[16] T. Nguyen, T. Dinh, A. R. M. Foisal, H.-P. Phan, T.-K. Nguyen, N.-T. Nguyen, and D. V. Dao, Nat. Commun. **10**(1), 4139 (2019).
[17] T. Nguyen, T. Dinh, J. Bell, V. T. Dau, N.-T. Nguyen, and D. V. Dao, ACS Appl. Mater. Interfaces **15**, 4294 (2022).
[18] A. R. M. Foisal, T. Dinh, V. T. Nguyen, P. Tanner, H.-P. Phan, T.-K. Nguyen, B. Haylock, E. W. Streed, M. Lobino, and D. V. Dao, IEEE Trans. Electron Devices **66**(4), 1804–1809 (2019).
[19] J. Chen, D. You, Y. Zhang, T. Zhang, C. Yao, Q. Zhang, M. Li, Y. Lu, and Y. He, ACS Appl. Mater. Interfaces **12**(48), 53957–53965 (2020).
[20] Z. Chen, Y. Wang, D. Zheng, F. Sun, X. Deng, Z. Tan, J. Tian, L. Zhang, M. Zeng, Z. Fan et al., J. Alloys Compd. **811**, 152013 (2019).
[21] A. M. Colomer, E. Massaguer, T. Pujol, M. Comamala, L. Montoro, and J. R. González, Appl. Energy **154**, 709–717 (2015).
[22] L. Y. Lou, J. Yang, Y. K. Zhu, H. Liang, Y. X. Zhang, J. Feng, J. He, Z. H. Ge, and L. D. Zhao, Adv. Sci. **9**(27), 2203250 (2022).
[23] H.-P. Phan, H.-H. Cheng, T. Dinh, B. Wood, T.-K. Nguyen, F. Mu, H. Kamble, R. Vadivelu, G. Walker, L. Hold et al., ACS Appl. Mater. Interfaces **9**(33), 27365–27371 (2017).
[24] A. R. M. Foisal, H.-P. Phan, T. Kozeki, T. Dinh, K. N. Tuan, A. Qamar, M. Lobino, T. Namazu, and D. V. Dao, RSC Adv. **6**(90), 87124–87127 (2016).
[25] T. Nguyen, D. Van Nguyen, H. Nguyen, B. Tong, C.-D. Tran, H. Takahashi, N.-T. Nguyen, D. V. Dao, and T. Dinh, T. Nguyen et al., "Light harvesting self-powered strain sensor using 3C-SiC/Si heterostructure," *2022 IEEE Sensors* (IEEE, Dallas, TX, 2022). pp. 1–4.
[26] S. O. Kasap, *Principles of Electronic Materials and Devices*, 4th ed. (McGraw-Hill Education, 2018).
[27] S. M. Sze, Y. Li, and K. K. Ng, *Physics of Semiconductor Devices* (John Wiley & Sons, 2006).
[28] T.-H. Nguyen, T. Nguyen, A. R. M. Foisal, T. A. Pham, T. Dinh, H.-Q. Nguyen, E. W. Streed, T.-H. Vu, J. Fastier-Wooller, P. G. Duran et al., ACS Appl. Electron. Mater. **4**(2), 768–775 (2022).